Flexible Shells

Theory and Applications

Edited by
E. L. Axelrad and F. A. Emmerling

With 107 Figures

Springer-Verlag
Berlin Heidelberg New York Tokyo 1984

Shallow Caps with a Localized Pressure Distribution Centered at the Apex[1]

FREDERIC Y. M. WAN[2]

Department of Mathematics and
Institute of Applied Mathematics and Statistics
The University of British Columbia
Vancouver, B.C. V6T 1W5
Canada

Introduction

Under favourable loading conditions, dome-shaped thin elastic shells of revolution are known to exhibit a predominantly inextensional bending deformation in the form of a finite axisymmetric dimple centered at the pole. For example, it has been shown in [1,2] that polar dimpling is possible when a spherical shell is subject to an axisymmetric normal pressure distribution which is directed inward near a pole and outward in an adjacent region[3]. To a good approximation, the dimple base radius, which characterizes the location of the dimple base and therefore the dimple size, was shown to depend on the external loading in a simple way. To bring out the essential idea behind the asymptotic method for constructing the simple solution, results for a spherical cap with a clamped edge were first presented in [1] for a quadratically varying pressure distribution along the shell meridian. Analogous and more general results were reported for a complete spherical shell in [2] for a meridionally sinusoidal pressure distribution.

The two approximate analyses in [1] and [2] both consist of showing the existence of two types of inextensional bending deformation which, when

(1) The research is partly supported by NSERC Operating Grant No. A9259. The author gratefully acknowledges Messrs. Derek Lee and Joseph Pang for their assistance in machine computation and computer graphics.

(2) The author is currently a Professor of Applied Mathematics and Mathematics in the Applied Mathematics Program, FS-20, University of Washington, Seattle, WA 98195, USA.

(3) This type of load distributions is of interest to the designers of fuel containers for space crafts and to biomechanicians and physiologists interested in biological structures involving fluid-filled thin shells (see [3] and [4] for examples).

pieced together by a bending layer solution, give an axisymmetric dimple centered at the pole. In the case of a shallow cap, the conditions of a support at the cap edge are satisfied by an edge bending layer solution. In the language of singular perturbations, (e.g., [19]), the inextensional bending solutions and the layer solutions correspond to the outer and inner asymptotic expansions, respectively, of the exact solution of the boundary value problem (BVP) governing the elastostatics of the shell. The main result in [1] and [2] is the simple determination of an accurate, first approximation dimple radius by way of the outer solutions of the BVP alone without any reference to the inner solution(s). Consistent with the spirit of this main result, the analyses in [1] and [2] also avoid the final matching of the inner and outer solutions. They rely on accurate numerical solutions of the original BVP to show the adequacy of the approximate location of the dimple base and of the outer solutions away from the dimple base and shell edge, for sufficiently thin shells and for a maximum applied inward pressure at least comparable to the classical buckling pressure for a spherical shell with the same radius of curvature. In a sequel to [1] soon to appear [5], the corresponding polar dimpling solution for general cap-like shallow shells of revolution under more general axisymmetric loadding conditions is obtained for a much wider range of maximum applied load magnitude. More precise conditions for the matching of inner and outer solutions are also given there.

To the extent that a detailed study of the more general polar dimpling solution obtained in [5] is presented there again only for a spherical cap with a quadratically varying pressure distribution (concentrating on the sub-buckling pressure magnitude range where dimples of two different sizes are possible), one of the purposes of this report is to complement the work of [5] and analyze in some detail the dimple solution for internally pressurized shallow caps with two types of localized axisymmetric inward applied loads important in engineering applications. These two types of localized loads have as their respective limiting case a point force at the pole and a ring load along a given lattitude. Beyond the dimple type deformations appropriate for the aforementioned applied loads, we will also discuss some typical load distributions for which nonlinear membrane action, instead of the inextensional bending action, dominates throughout the shallow cap except in some narrow interior and/or edge layers. The report concludes with some comments on a class of axisymmetric load distributions

of interest to engineers which may give rise to one of the two kinds of nonlinear membrane behaviours, or to a dimple type inextensional bending behaviour, depending on the relative magnitude of the several load and geometric parameters.

Formulation

The elastostatics of shells of revolution, which have undergone an axisymmetric finite deformation (with infinitesimal strain), may be formulated as a boundary value problem for a pair of coupled nonlinear second order ordinary differential equations for a stress function and a meridional slope variable [6]. Let x $(0\le x\le 1)$ denote the dimensionless radial distance from the axis of revolution to a point on the middle surface of a cap-like shallow shell of revolution having uniform thickness h. We consider here shells subjected to a general axisymmetric (positive inward) normal load distribution $p_n = p_v p(x)$, with p_v chosen so that the dimensionless resultant axial force P (defined in (2.3)) is $O(1)$[4], and a genereral axisymmetric (positive outward) radial surface load distribution $p_r = p_H q(x)$ (with $|q|_{max} = 1$). With an undeformed meridional slope $\xi_0\Phi_0(x)$ $(\Phi_0(1) = 1)$, we may take these equations in the following dimensionless form [7]:

$$\varepsilon^2 x[\Psi'' + \frac{1}{x}\Psi' - \frac{1}{x^2}\Psi] + \frac{1}{2}(\Phi^2 - \Phi_0^2) = -4\mu x[xq' + (2+\nu)q] \qquad (2.1)$$

$$\varepsilon^2 x[\Phi'' + \frac{1}{x}\Phi' - \frac{1}{x^2}\Phi] - \Phi\Psi = 4\kappa x P(x) + \varepsilon^2 x Q(x) \qquad (2.2)$$

with

$$P(x) = \frac{1}{x}\int_0^x tp(t)dt, \qquad (2.3)$$

$$Q(x) = \Phi_0'' + \frac{1}{x}\Phi_0' - \frac{1}{x^2}\Phi_0. \qquad (2.4)$$

(4) p may be unbounded in the limiting case of a point load or ring load.

In (2.1)-(2.4), a prime indicates differentiation with respect to x, $\xi_0\Phi(x)$ denotes the meridional slope of the deformed middle surface of the shell, and the dimensionless independent variable x is related to the radial distance from the axis of revolution $r(0\le r\le r_0)$ by $x = r/r_0$ (see Fig. 1). In terms of r_0, the shell thickness h, Young's modulus E, Poisson's ratio ν, and the radius of curvature measure of the shell $a = r_0/\xi_0$, we have

$$\varepsilon^2 = \frac{ha}{2r_0^2\sqrt{3(1-\nu^2)}}, \qquad \mu = \frac{h}{2r_0\sqrt{3(1-\nu^2)}}\frac{p_H}{p_c}$$

$$\kappa = \frac{p_v}{p_c}, \qquad p_c = \frac{2Eh^2}{a^2\sqrt{3(1-\nu^2)}} \qquad (2.5)$$

We note also that the dimensionless stress function Ψ is the conventional stress function normalized by $p_c a r_0/4$ with $p_c a\Psi/4x$ and $p_c a\Psi'/4$ being the radial and hoop stress resultant, respectively.

Equations (2.1) and (2.2) are supplemented by the regularity conditions at the apex:

$$x = 0: \qquad \Phi = 0, \qquad \Psi = 0, \qquad (2.6)$$

and appropriate edge conditions depending on the type of support for the shell at $x = 1$. For example, we consider in sections (3) - (5) shells with a clamped edge so that

$$x = 1: \qquad \Phi = 1, \qquad \Psi' - \nu\Psi = 0, \qquad (2.7)$$

though our analysis applied to shells with other types of edge support, possibly after suitable (but straightforward) modifications. The second condition in (2.7) corresponds to a requirement of no radial midsurface displacement. A discussion of other stress and deformation measures of the shallow shell can be found in [1,2,6,7].

For the most part of this report, we shall be concerned mainly with the simpler problem of a spherical cap, $\Phi_0(x) = x$, subjected only to a

dimensionless axisymmetric normal pressure load distribution of the form

$$p(x) = \begin{cases} -p_2 & (0 \le x < x_1) \\ -p_2 + \dfrac{P_1}{(x_2^2-x_1^2)} & (x_1 < x < x_2) \\ -p_2 & (x_2 < x \le 1) \end{cases} \qquad (2.8)$$

with the corresponding axial resultant given by

$$P(x) = \begin{cases} -\frac{1}{2} p_2 x & (0 \le x \le x_1) \\ -\frac{1}{2} p_2 x + \frac{P_1}{2x} \dfrac{x^2-x_1^2}{x_2^2-x_1^2} & (x_1 \le x \le x_2) \\ -\frac{1}{2} p_2 x + \frac{P_1}{2x} & (x_2 \le x \le 1) \end{cases} \qquad (2.9)$$

For this special case, the ODEs (2.1) and (2.2) become (with $q(x)\equiv 0$)

$$\varepsilon^2 x[\psi'' + \frac{1}{x}\psi' - \frac{1}{x^2}\psi] + \frac{1}{2}(\Phi^2-x^2) = 0, \qquad (2.10)$$

$$\varepsilon^2 x[\Phi'' + \frac{1}{x}\Phi' - \frac{1}{x^2}\Phi] - \Phi\psi = 4\kappa x P(x), \qquad (2.11)$$

$(0<x<1)$

where $P(x)$ is as given by (2.9). Note that $\pi r_0 p_v P_1$ is the dimensionless resultant force associated with the annular normal pressure distribution when $p_2 = 0$. Upon specializing the four parameters at our disposal, namely, p_2, P_1, x_1 and x_2, we get from (2.8) and (2.9) a variety of load conditions useful in engineering applications. We shall analyze the behaviour of shells under these external loads in the next few sections.

Internally Pressurized Caps with a Patch Load at the Apex

For $x_1 = 0$ and $0<x_2<<1$, the applied load (2.8) corresponds to a uniform internal pressure (of dimensionless magnitude $-p_2$) throughout the shell and a localized (axi-symmetric) uniform external pressure centered at the pole with a magnitude inversely proportional to its area of application.

For the net pressure to be inward near the pole, we take $P_1>p_2x_2^2$. Note that the magnitude of the resultant force associated with the external pressure is independent of the area of application. In the limit as $x_2 \to 0$, we have an internally (uniformly) pressurized cap with a point force at its pole. In the absence of internal pressure ($p_2=0$) and radial load ($q(x)\equiv 0$), the problem has been investigated in [8-16] and elsewhere. In this section, we are concerned with the case $q(x) = 0$ but $p_2 \neq 0$ for shells with a clamped edge and sufficiently thin so that $\varepsilon^2<<1$.

When κ is O(1) or larger with $\kappa\varepsilon^2<<1$, we know from [1,2,5] that polar dimpling is a possible mode of deformation. The dimple solution consists of the inextensional bending solutions

$$[\Phi,\Psi] \sim \begin{cases} [-\Phi_0,\ 4\kappa x P/\Phi_0] & (0 \le x < x_T) \\ [\Phi_0,\ -4\kappa x P/\Phi_0] & (x_T < x < 1) \end{cases} \qquad (3.1)$$

in two disjoint regions of the shell, an interior layer solution in the neighborhood of x_T to bridge them and a boundary layer solution adjacent to the shell edge to satisfy the clamped edge conditions (2.7). The leading term outer solutions (3.1) are obtained by setting to zero the small parameter ε in the two ODEs (2.1) and (2.2), assuming $xP(x)/\Phi_0(x)$ is well defined in [0,1] except at $x = x_T$. Cases where the shell has a horizontal tangent and/or a flat point have already been treated separately in [17]. We also do not concern ourselves here with the layer solutions, though their presence will be seen from the graphs of the numerical solutions to be shown and discussed at the end of the section. Note that our choice of outer solutions in the two disjoint regions of the shallow cap anticipates the occurrence of the dimpling phenomenon.

The dimensionless dimple base radius x_T is determined to a first approximation by the requirement of vanishing axial resultant to be a positive root $\bar{x}_t$ of $P(x) = 0$. This requirement is a necessary condition for the existence of the interior layer (or the inner) solution for bridging the two types of inextensional bending (or outer) solutions [5]. Physically, it renders the radial stress resultant continuous across the dimple base. For the $P(x)$ under consideration, there is always a single positive root (since we consider only the range $P_1 \ge p_2 x_2^2$) with

$$x_T \sim \bar{x}_t \equiv \sqrt{\frac{P_2}{p_2}} \geq x_2 \qquad (3.2)$$

($P(x)$ never vanishes except at $x = 0$ if $P_1 \leq p_2 x_2^2$ so that polar dimpling is not possible in that range of parameter values.) It is rather remarkable that to leading order, the dimple size depends only on the applied load and not on the shape, thickness or material properties of the shell, at least when the shell is sufficiently thin (and $\kappa >> \varepsilon$).

Accurate numerical solution for the BVP of (2.1), (2.2), (2.6) and (2.7) have been obtained by the BVP solver COLSYS [18], a general purpose computer code for solving ODEs with prescribed boundary values at the end (and/or intermediate) points of the solution domain. Based on spline-collocation at Gaussian points with error estimates, the codes solves a given problem on a sequence of meshes, automatically increasing the number of mesh points in region of abrupt changes, until the solution obtained meets a prescribed (combination of absolute and relative) error tolerance, or until the prescribed maximum mesh is reached without meeting the error tolerance. Some of these accurate numerical solutions are presented here for comparison with the asymptotic solution (3.1) and (3.2). For this purpose, we show only results for a shallow spherical cap with $\Phi_0(x) = x$ and with $\nu = 0.3$.

In Figure (2), we show distributions of the deformed slope $\Phi(x)$ for $\varepsilon^2 = 10^{-4}$, $\kappa = 1$, and $\bar{x}_t \equiv \sqrt{P_1/p_2} = 3/4$, each curve corresponding to a different value of x_2, i.e., a different size of application area (and a different magnitude) of the localized external pressure. These numerical results, generated by COLSYS for the BVP defined by (2.6), (2.7), (2.9)-(2.11), clearly show in all cases a dimple type deformation pattern with an identical dimple radius independent of x_2, a phenomenon predicted by our asymptotic solution (see (3.2)). The (approximate) dimple radius $\bar{x}_T$ as given by COLSYS, i.e. the location where the COLSYS solution for Φ vanishes, agrees with the asymptotic solution $\bar{x}_t$ to within 5%. It should be noted that all COLSYS results presented in this paper have met a prescribed error tolerance of 10^{-4} (and often smaller).

In Figure (3), three COLSYS solutions for $\Phi(x)$ are given for $\kappa = 1$, $x_2 = 0.1$ and $\bar{x}_t = \sqrt{P_1/p_2} = 3/4$; they correspond to three different thickness parameter values, $\varepsilon^2 = 10^{-3}$, 10^{-4} and 10^{-5}. We see from these plots that,

in all cases, the dimple sharpens and the layer width decreases as ε decreases. They also show that as ε decreases $\bar{x}_t$ approaches $\bar{x}_T$, the COLSYS solution for x_T.

In Figure (4), three COLSYS solutions for $\Phi(x)$ are given for $x_2 = 0.05$, $\varepsilon^2 = 10^{-4}$ and $\kappa = 1$; they correspond to $\sqrt{P_1/p_2} = 0.4$, 0.6 and 0.75. The figure shows that the dimple size depends only on the ratio P_1/p_2 according to (3.2) to a first approximation.

Other numerical solutions not presented here show that the sharpness of the dimple solution deteriorates as κ increases. It is known from [5] that nonlinear membrane shell action becomes more significant as κ becomes much larger than unity. Our numerical solutions show that it completely dominates the inextensional bending shell action when $\kappa\varepsilon^2 \gtrsim 1$ for the present problem.

At the other end of the spectrum, we also know from [5] that, when κ is small of order ε, say $\kappa = k\varepsilon$ with $k = O(1)$, the necessary condition for the existence of an interior layer solution takes the form

$$4\kappa P(x_T) = \varepsilon I_0 + O(\varepsilon^2) \qquad (3.3)$$

where I_0 is a pure number for a spherical cap ($I_0 \simeq 1.6674...$). Therefore, we have to a first approximation

$$P_1 - p_2 \bar{x}_t^2 = \frac{I_0}{2k} \bar{x}_t \qquad (3.4)$$

in the case of $\kappa = k\varepsilon$. In contrast to the case of a quadratically varying pressure load distribution [5] which allows for two different dimple radii, the size of the dimple remains unique in this "sub-buckling" range of the localized load at the pole. Furthermore, for the localized load at the pole, the condition (3.3) always has a unique positive solution for all $k > 0$. We should note, however, that (3.3) ceases to be valid if $k = O(\varepsilon)$ (see the derivation of (3.3) in [5]) and is raplaced by $I_0 + O(\varepsilon) = 0$ instead. Therefore, polar dimpling is not possible for the type of applied loads considered in this section when $\kappa = O(\varepsilon^2)$ since the necessary condition for the existence of an interior layer solution (which bridges the two outer solutions given in (3.1)) cannot be satisfied. From Figure (5), we

see that the dimple radius shrinks continuously from O(1) to O(ε) as k decreases from O(1) to O(ε). However, the form of P(x) requires $\bar{x}_t \geq x_2$ giving a lower bound to the possible size of the dimple.

Finally, we note that all COLSYS solutions for $\Phi(x)$ display a layer phenomenon in the neighborhood of the load discontinuity at x_2 (see (2.8) with $x_1 = 0$). The bending layer is generated as neither membrane nor inextensional bending shell action could absorb the abrupt changes caused by the load discontinuity.

Internally Pressurized Caps with an Axi-symmetric Ring Load

For $0 < x_2 - x_1 << 1$ with $x_1 > 0$, the load distribution (2.8) corresponds to a uniform internal pressure throughout the shell and a localized uniform external pressure distributed axisymmetrically over an annular frustum of the shell (extending from x_1 to x_2) with a magnitude inversely proportional to the area of application. In the limit as $x_2 - x_1 \to 0$, we have an internally pressurized cap with a ring load at the lattitude $x = x_1 (=x_2)$. In the absence of the internal pressure ($p_2 = 0$) and radial load ($q(x) \equiv 0$), the problem has been investigated previously in [14] and elsewhere. In this section, we are concerned with the case $q(x) \equiv 0$ but $p_2 \neq 0$ for sufficiently thin shells so that $\varepsilon^2 << 1$.

For κ not small compared to unity but $\kappa\varepsilon^2 << 1$, we expect the possibility of polar dimpling. The condition $P(x) = 0$, determining x_T to a first approximation, now implies the following:

(1) Polar dimpling is not possible for $P_1 < p_2 x_2^2$, similar to the case of a patch load at the apex.

(2) There is a unique dimple size when $P_2/p_2 = x_2^2$, namely $\bar{x}_t = x_2$.

(3) For $P_1 > p_2 x_2^2$, $P(x) = 0$ has two distinct positive roots given by

$$\bar{x}_t = \begin{cases} x_1/[1 - p_2(x_2^2 - x_1^2)/P_1]^{1/2} \equiv \bar{x}_t^{(1)} & (x_1 < \bar{x}_t^{(1)} < x_2) \\ \sqrt{P_1/p_2} \equiv \bar{x}_t^{(2)} & (>x_2) \end{cases} \tag{4.1}$$

For $P_1/p_2 > x_2$, the existence of two dimple base radii offers a number of possible configurations for the deformed shells. For example, one may have a large dimple corresponding to $\bar{x}_t^{(2)}$ or a small dimple corresponding to $\bar{x}_t^{(1)}$. From an analytical viewpoint, the admissable configurations are ultimately determined by matching the inextensional bending solutions and the various layer solutions. We will not carry out this matching process here since the following outer solution is readily suggested by our particular load distribution:

$$\Phi \sim \begin{cases} \Phi_o(x) & (0 \leq x < x_T^{(1)}) \\ -\Phi_o(x) & (x_T^{(1)} < x < x_T^{(2)}) \\ \Phi_o(x) & (x_T^{(2)} < x < 1) \end{cases} \tag{4.2}$$

with the corresponding Ψ given by $-4\kappa x P/\Phi$. We also expect that, to a first approximation, we have

$$x_T^{(1)} \sim \bar{x}_t^{(1)} \quad , \qquad x_T^{(2)} \sim \bar{x}_t^{(2)} \tag{4.3}$$

Note that $\bar{x}^{(1)}$ decreases from x_2 as P_1 increases (or p_2 decreases), tending to its lower bound x_1. On the other hand $\bar{x}_t^{(1)}$ approaches x_2 as P_1 decreases; $\bar{x}_t^{(1)}$ and $\bar{x}_t^{(2)}$ coalesce as P_1 tends to $p_2 x_2^2$ from above.

The expression (4.2) is confirmed to be the leading term outer solution for $\varepsilon << 1$ by the COLSYS solutions for $\Phi_o(x) = x$ and $\nu = 0.3$ given in Figures (6) and (7). In Figure (6), we have three COLSYS solutions for $\Phi(x)$ for $\kappa = 1$, $x_1 = 0.3$, $x_2 = 0.4$, $P_1 = 1$ and $p_2 = 16/9$ (so that $\bar{x}_t^{(2)} = 0.75$ and $\bar{x}_t^{(1)} = 0.3206$); they correspond to $\varepsilon^2 = 10^{-3}$, 10^{-4}, and 10^{-5}. While the COLSYS solution is numerically close to the solution (4.2) only for the smallest ε, the two locations of horizontal tangent in the deformed shell shape, $\bar{x}_T^{(1)}$ and $\bar{x}_T^{(2)}$, are nearly indistinguishable from $\bar{x}_t^{(1)}$ and $\bar{x}_t^{(2)}$, respectively, in all three cases. Figure (7) also displays three COLSYS solutions for $\Phi(x)$ for $\kappa = 1$, $x_1 = 0.4$, $\varepsilon^2 = 10^{-4}$, $P_1 = 1$ and $p_2 = 16/9$; they correspond to $x_1 = 0.1$, 0.25 and 0.39 (with $\bar{x}_t^{(1)} = 0.1168$, 0.2750, and 0.3928, respectively). They show that (4.2) continues to be a good approximation for (the COLSYS) $\Phi(x)$ whether the spread of the external pressure is wide or

narrow and that $x_t^{(2)}$ is unaffected by the width of the spread. In general, COLSYS always converges to a solution with the qualitative features of (4.2) if $\varepsilon^2 \lesssim 10^{-2}$, whatever the initial guess of the solution may be.

Whenever polar dimpling is possible, the qualitative features of the dimple solution are similar to the point load case. The dimple base radius $x_t^{(2)} \sim \bar{x}_t^{(2)} \equiv \sqrt{P_1/p_2}$ is asymptotically independent of the size of the area over which the external pressure distributes. The nonlinear membrane action again dominates when $\kappa\varepsilon^2$ is <u>not</u> small compared to unity, with the dimple deteriorates gradually as κ tends to ε^{-2}. At the other end of the spectrum, the dependence of $\bar{x}_t^{(2)}$ on κ in the range $\kappa = O(\varepsilon)$, say $\kappa = k\varepsilon$, is again similar to the point force case discussed previously. In particular, the asymptotic value of $\bar{x}_t^{(2)}$ decreases to x_2 as k decreases from O(1) to o(1), while $x_t^{(1)}$ increases to x_2; the dimple disappears as $x_t^{(1)}$ and $x_t^{(2)}$ coalesce. Polar dimpling is again not possible if k is of order ε or smaller.

<u>Shallow Caps with a Ring of Internal Pressure</u>

Consider now the case of $p_2 = 0$, and $q(x) \equiv 0$ and $P_1 < 0$ so that the shell is subject only to an internal pressure distributed over an annular region of the shell. The magnitude of the applied pressure is sufficiently high so that $\kappa\varepsilon^2$ is <u>not</u> small compared to unity. In this range, the nonlinear membrane action dominates throughout the shell except for some narrow layers. Anticipating this non-linear membrane behaviour, we set

$$\psi = \frac{\kappa^{2/3}}{\varepsilon}\psi \quad , \qquad \Phi = (\kappa\varepsilon^2)^{1/3}\phi \tag{5.1}$$

and write the ODE (2.1), (2.2) and the boundary conditions (2.6), (2.7) as

$$x[\psi'' + \frac{1}{x}\psi' - \frac{1}{x^2}\psi] + \frac{1}{2}[\phi^2 - (\kappa\varepsilon^2)^{-2/3}\phi_0^2] = 0 \tag{5.2}$$

$$\varepsilon^4(\kappa\varepsilon^2)^{-2/3}x[\phi'' + \frac{1}{x}\phi' - \frac{1}{x^2}\phi] - \phi\psi = 4xP(x) + \varepsilon^4(\kappa\varepsilon^2)^{-1}xQ(x) \tag{5.3}$$

with

$$x = 0: \qquad \phi = 0, \qquad \psi = 0, \tag{5.4}$$

$$x = 1: \qquad \phi = (\kappa\varepsilon^2)^{-1/3} \quad \psi' - \nu\psi = 0 \tag{5.5}$$

With $(\kappa\varepsilon^2)^{-2/3} = O(1)$ at most, the leading term outer solution of the BVP for $\varepsilon^2 \ll 1$, denoted by ϕ_0 and ψ_0, is determined by

$$\phi_0\psi_0 = -4xP(x) \tag{5.6}$$

along with (5.2), (5.4) and (5.5) (in which ϕ_0 and ψ_0 take the place of ϕ and ψ, respectively). For simplicity, we shall discuss the solution process only for a spherical cap with $x_1 = x_2$. The annular pressure load thus takes its limiting form of a ring load with

$$-4xP(x) = \begin{cases} 0 & (0 \le x < x_1) \\ -2P_1 & (x_1 < x \le 1) \end{cases} \tag{5.7}$$

where $P_1 < 0$. The method, with some straightforward modifications, also applies to the case $x_1 < x_2$ and more general shell shape $\Phi_0(x)$.

In the range $0 < x < x_1$, the algebraic equation (5.6) with the right hand side given by (5.7) may be satisfied by either $\phi_0(x) \equiv 0$ or $\psi_0(x) \equiv 0$. For the solution to be applicable for both moderate and large values of $\kappa\varepsilon^2$, we take

$$\phi_0(x) \equiv 0 \ (\equiv\hat{\phi}_p(x)) \quad (0 \le x < x_1) \tag{5.8}$$

which automatically satisfies the first boundary condition in (5.4). With (5.8), the shell is flattened out in the neighborhood of the pole (as we would expect for a sufficiently high pressure magnitude). Corresponding to this mode of deformation, we have from (5.2) (with $\phi_0^2 = x^2$)

$$[\psi_0'' + \frac{1}{x}\psi_0' - \frac{1}{x^2}\psi_0] = \frac{1}{2}(\kappa\varepsilon^2)^{-2/3}x, \quad (0 \le x < x_1). \tag{5.9}$$

The solution of (5.9) satisfying the second condition of (5.4) is

$$\psi_0(x) = A_1x + \frac{1}{16}(\kappa\varepsilon^2)^{-2/3}x^3 \equiv \hat{\psi}_p(x) \quad (0 \le x < x_1). \tag{5.10}$$

(With both regularity conditions at x = 0 satisfied, there will be no layer solution in the neighborhood of the apex.) The remaining constant of integration A_1 is to be determined by the matching of $\hat{\psi}_p(x)$ and $\hat{\phi}_p(x) \equiv 0$

with an appropriate layer (inner) solution in the neighborhood of x_1.

For the range $x_1 < x < 1$, we have from (5.6)

$$\phi_0 = -\frac{2P_1}{\psi_0}, \quad (x_1 < x < 1) \tag{5.11}$$

so that (5.2) (with $\phi_0^2(x) = x^2$) may be written as

$$x[\psi_0'' + \frac{1}{x}\psi_0' - \frac{1}{x^2}\psi_0] + \frac{2P_1^2}{\psi_0^2} = \frac{1}{2}(\kappa\varepsilon^2)^{-2/3}x^2, \quad (x_1 < x < 1). \tag{5.12}$$

The solution of this second order ODE, denoted by $\hat{\psi}_e(x)$, cannot be made to satisfy the two boundary conditions at $x = 1$ given by (5.5) as well as matching with the layer solution in the neighborhood of x_1. A boundary layer (inner) solution adjacent to the shell edge is needed to satisfy the boundary conditions. The two constants of integration of $\hat{\psi}_e$ and the arbitrary constant A_1 in $\hat{\psi}_p$ are determined by matching the outer solutions $\hat{\psi}_p$ and $\hat{\psi}_e$ with the inner solutions, one in the neighborhood of x_1 and the other adjacent to the shell edge.

Analyses of the structure of the interior layer at $x = x_1$, and the boundary layer at $x = 1$ (details of which will not be included here) show that only ϕ changes abruptly over a small distance along a shell meridian in these layers. The corresponding matching of the inner and outer solutions effectively requires $\hat{\psi}_e$ to satisfy

$$\hat{\psi}_e'(1) - \nu\hat{\psi}_e(1) = 0, \tag{5.13}$$

i.e., the "no radial displacement" condition in (5.6), and

$$x = x_1: \quad x\hat{\psi}_e' - \hat{\psi}_e = \frac{1}{8}(\kappa\varepsilon^2)^{-2/3}x^3, \tag{5.14}$$

with the only unknown constant A_1 in $\hat{\psi}_p(x)$ given by

$$A_1 = \hat{\psi}_e'(x_1) - \frac{3}{16}(\kappa\varepsilon^2)^{-2/3}x_1^2 \tag{5.15}$$

(The conditions (5.14) and (5.15) effectively ensure $\hat{\psi}_p(x_1) = \hat{\psi}_e(x_1)$ and $\hat{\psi}_p'(x_1) = \hat{\psi}_e'(x_1)$.) The solution procedure at this point is to solve the

two point BVP defined by (5.12)-(5.14) to determine $\hat{\psi}_e(x)$, $x_1 \le x \le 1$ and then use (5.15) to calculate A_1, thereby completely determining $\hat{\psi}_p(x)$, $0 \le x \le x_1$.

There still remains the formulation of appropriate BVP for the two layer solutions. We shall not be concerned with this aspect of the problem as the stresses associated with the layer solutions are at most comparable to membrane stresses associated with $\hat{\psi}_p(x)$ and $\hat{\psi}_e(x)$. We merely note that the interior layer solution mainly serves to smooth out the discontinuity of the two different outer solutions for $\phi(x)$ across x_1, while the boundary layer solution ensures the condition of no rotation, $\phi(1) = \phi_0(1)$, at the shell edge.

When $\phi_0(x) \equiv 0$, the nonlinear ODE (5.12) for $\hat{\psi}_e$ is the governing equation in the Föppl-Hencky (small finite-deflection) nonlinear theory of an originally flat elastic membrane [20,21]. Existence, uniqueness and numerical methods of the solution for this ODE in the case of annular membranes with various stress and displacement boundary conditions, including (5.13), have been reported in [22] and other references cited therein. Numerical solutions of (5.12) with (5.14) taking the place of a conventional boundary condition at the inner edge pose no new difficulties. These solutions along with (5.11), (5.8), (5.10) and (5.15) (henceforth called nonlinear membrane solutions) give the limiting behaviour of the shell for very small values of ε.

Figure (8) shows three COLSYS solutions for $\phi(x)$ for shells with a ring of uniform internal pressure extending from $x_1 = 0.5$ to $x_2 = 0.51$; they are for $\varepsilon^2 = 10^{-1}$, 10^{-2} and 10^{-4} with the corresponding pressure magnitude given by $P_1 = -1$ and $\kappa = \varepsilon^{-2}$ (or $\kappa\varepsilon^2 = 1$). These distributions of $\phi(x)$ show clearly that the shells exhibit mainly nonlinear membrane action and that their deformed meridional slope $\phi(x)$ tends to $(\kappa\varepsilon^2)^{1/3}\phi_0(x)$ as ε becomes smaller and smaller. For $\varepsilon^2 = 10^{-4}$, the COLSYS solution differs by less than 5% from the limiting nonlinear membrane solution throughout the shell except in the two narrow layers of abrupt changes located around $x = x_1$ and $x = 1$. It is remarkable that the rather complex and nearly discontinuous distribution of $\phi(x)$ for $\varepsilon^2 \ll 1$ can be so accurately generated by COLSYS. It is even more remarkable that a simple outer asymptotic solution, which completely describes the limiting behaviour for shells with

vanishing thickness, may be obtained from (2.1) and (2.2) by setting $\varepsilon = 0$ after re-scaling these ODEs (and then using technique of matched asymptotic expansions or physical reasoning).

The agreement between the COLSYS solution for the shell and the limiting nonlinear membrane solution is even better and extends to the edge of the shell ($x = 1$) if the shell is hinged (so that the condition $\phi = \phi_0$ in (2.7) is replaced by $\phi' + \nu\phi = \phi_0' + \nu\phi_0$) at the edge instead (as shown in Figure (9)). We show in Figure (9) two solutions for $\phi(x)$ for shells with a clamped edge and with $\varepsilon^2 = 10^{-2}$, $\kappa\varepsilon^2 = 1$, $P_1 = -1$; they correspond to a ring pressure load at the two different locations, namely ($x_1 = 0.5$, $x_2 = 0.51$) and ($x_1 = 0.75$, $x_2 = 0.76$). Also shown there are the corresponding two solutions when the shell is hinged at $x = 1$ instead. The qualitative features of $\phi(x)$ (outside the narrow layers of abrupt changes) as shown in Figure (8) remain unaffected by the change in the location of the ring load and the type of edge conditions.

Finally, Figure (10) shows the effect of the ring load spread ($x_2 - x_1$) by the COLSYS solutions for ($x_2 - x_1$) = 0.01, 0.1 and 0.25 and for $x_1 = 0.5$. The change from a flat region in the deformed configuration (given by (5.8), (5.10) and (5.15)) to a nearly conical region (given by (5.11) - (5.14)) is much more gradual for a wider load spread. Over the region of the pressure ring ($x_1 \le x \le x_2$), the deformed shape of the shell continues to be spherical but with a smaller spherical radius.

Concluding Remarks

In this report, we have considered only shells subject to axial loads. For the more general situation of combined axial and radial loads, the possible modes of shell behaviour generally depends on the relative magnitude of the two types of loadings. This dependence on load magnitude is evidently more complicated than what we have encountered in this report for shells subject only to axial loads. A complete analysis of this dependence can be found in [23]. When subjected only to radial loads, however, we know from [24] that a very thin shell behaves effectively as a membrane except near an edge support and that a nonlinear membrane solution is often needed for a correct description of the qualitative behaviour of the shell even for very small radial load magnitudes.

References

1. Wan, F.Y.M.: The dimpling of spherical caps. Mechanics Today 5: The Eric Reissner Anniversary Volume (1980) 495-508.

2. _____; Polar dimpling of complete spherical shells, Theory of Shells, Proc. of the Third IUTAM Shell Symp. (Tbilisi, USSR; August, 1978), Ed. W.T. Koiter & G.K. Mikhailov, North-Holland, 1980, 589-605.

3. Bucciarelli, L.L.: The analysis of propellant expulsion bladders and diaphrams. Dept. of Aero. & Astro. Tech. Rep., M.I.T., Cambridge, MA., 1967.

4. Taber, L.A.: Large deflection of a fluid-filled spherical shell under a point load. J. Appl. Mech. 49 (1982) 121-128.

5. Parker, D.F.; Wan, F.Y.M.: Finite polar dimpling of shallow caps under sub-buckling pressure loading. (I.A.M.S. Tech. Rep. No. 80-10, U.B.C., Vancouver, Canada and) SIAM J. Appl. Math (1984) to appear.

6. Reissner, E.: On Axisymmetric deformations of thin shells of revolution. Proc. Symp. in Appl. Math., III, Amer. Math. Soc., Providence (1950) 27-52.

7. _____: Symmetric bending of shallow shells of revolution. J. Math. Mech. 7 (1958) 121-140.

8. Ashwell, D.G.: On the large deflexion of a spherical shell with an inward point load. Proc. First Symp. on Thin Elastic Shells (Delft, The Netherlands; August, 1959), Ed. W.T. koiter, North-Holland, Amsterdam (1960) 43-63.

9. Archer, R.R.: On the numerical solution of the nonlinear equations of shells of revolution. J. Math. & Phys. 41 (1962) 165-178.

10. Evan-Iwanowski, R.M.; Cheng, H.S.; Loo, T.C.: Experimental investigations of deformations and stability of spherical shells subjected to concentrated load at the apex. Proc. 4th U.S. Nat'l Congr. Appl. Mech. (1962) 563-575.

11. Penning, F.A.; Thurston, G.A.: The stability of shallow spherical shells under concentrated load. NASA CR-265, July, 1965.

12. Mescall, J.F.: Large deflections of spherical shells under concentrated loads. J. Appl. Mech. 32 (1965) 936-938.

13. Penning, F.A.: Experimental buckling modes of clamped shallow shells under concentrated load. J. Appl. Mech. 33 (1966) 297-304.

14. Bushnell, D.: Bifurcation phenomena in spherical shells under concentrated and ring loads. AIAA J. 5 (1967) 2034-2040.

15. Fitch, J.R.: The buckling and post-buckling behavior of spherical caps under concentrated load. Int'l J. Solids & Structures 4 (1968) 421-446.

16. Ranjan, C.V.; Steele, C.R.: Large deflection of deep spherical shells under concentrated load, Proc. AIAA/ASME 18th Structures, Structural Dynamics and Materials Conf. (San Diego, Calif.; March, 1977), 269-278.

17. Wan, F.Y.M.; Ascher, U.: Horizontal and flat points in shallow shell dimpling. Proc. of BAIL I Conf. (Dublin, 1980), Ed. J. Miller, Boole Press, Dublin, 1980, 659-679.

18. Ascher, U; Christiansen, J; Russell, R.D.: A collocation solver for mixed order systems of boundary value problems. Math. Comp. 33 (1979) 659-679.

19. Kevorkian, J.; Cole, J.D.: Perturbation methods in Applied Mathematics, Springer-Verlag, New York-Heidelberg-Berlin, 1981.

20. A. Föppl, Vorlesungen über technische Mechanik, Vol. III, Teubner, Leipzig, 1907.

21. Hencky, H.: Über den spannungzustaud in kreisrunden platten mit verschwindender biegungssteifigkeit. Z.f. Math. u. Phys. 63 (1915) 311-317.

22. Weinitschke, H.J.: On axisymmetric deformations of nonlinear elastic membranes. Mech. Today 5: E. Reissner Anniversary Volume (1980) 523-542.

23. Lin, Y.H.; Wan, F.Y.M.: Asymptotic solutions of steadily spinning shallow shells of revolution under uniform pressure. I.A.M.S. Tech. Rep. No. 83-25, U.B.C., Vancouver, Canada.

24. Reissner, E.; Wan, F.Y.M.: Rotating shallow elastic shells of revolution. J. of S.I.A.M. (now S.I.A.M. J. of Appl. Math.) 13 (1965) 333-352.

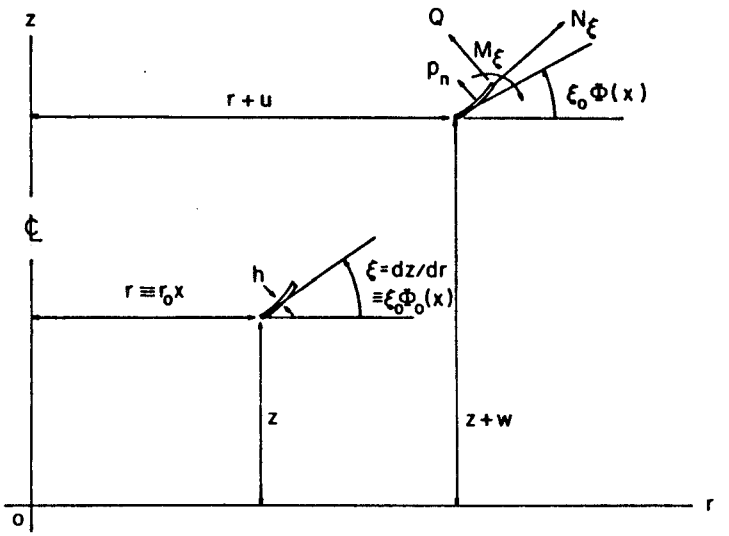

Figure 1. Dome-shaped Shallow Shells of Revolution

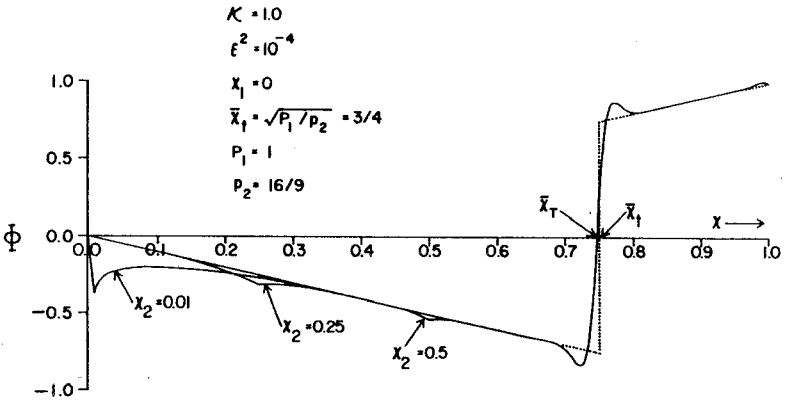

Figure 2. Distributions of Deformed Meridional Slope for Different Localized External Pressure Distributions with the Same Resultant

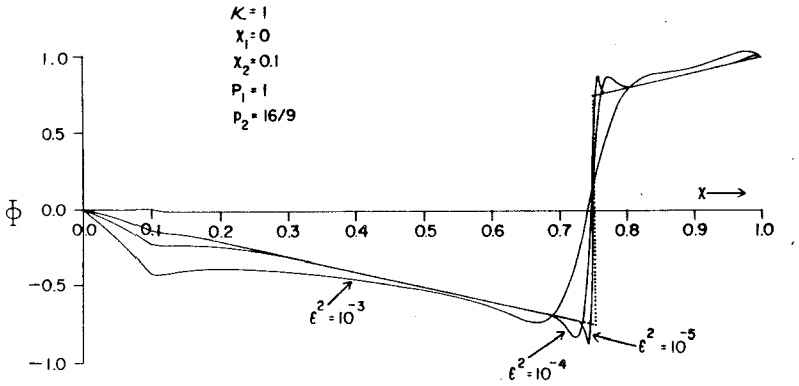

Figure 3. Distributions of Deformed Meridional Slope of Shells with Different Thickness Parameter Values Subjected to the Same Localized Load

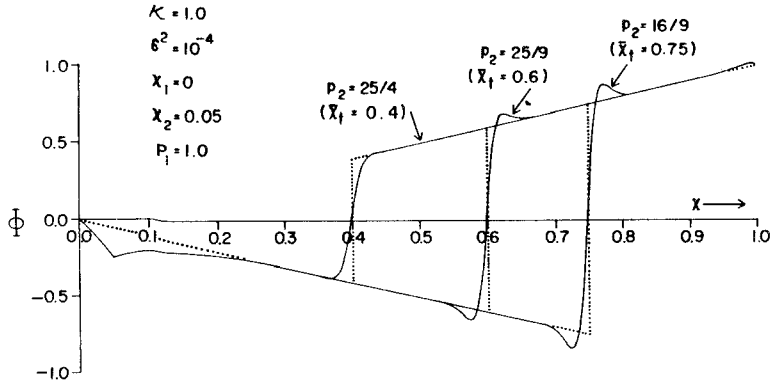

Figure 4. Distributions of Deformed Meridional Slope for Shells with the Same Localized Distribution External Pressure but with Different Internal Pressures

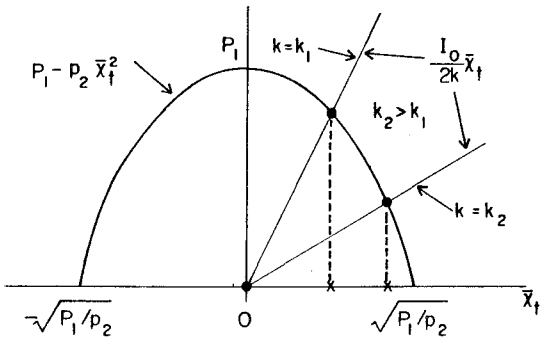

Figure 5. The Variation of Dimple Radius with Load Magnitude for $\kappa = \kappa\varepsilon$

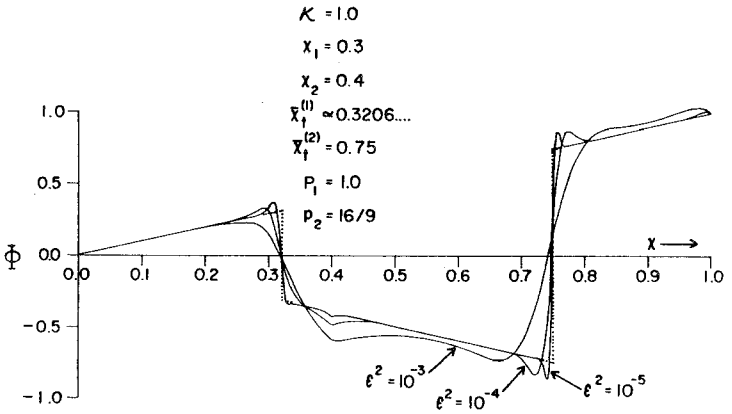

Figure 6. Distributions of Deformed Meridional Slope for Shells with the Same External Ring Pressure but Different Thickness Parameter Values

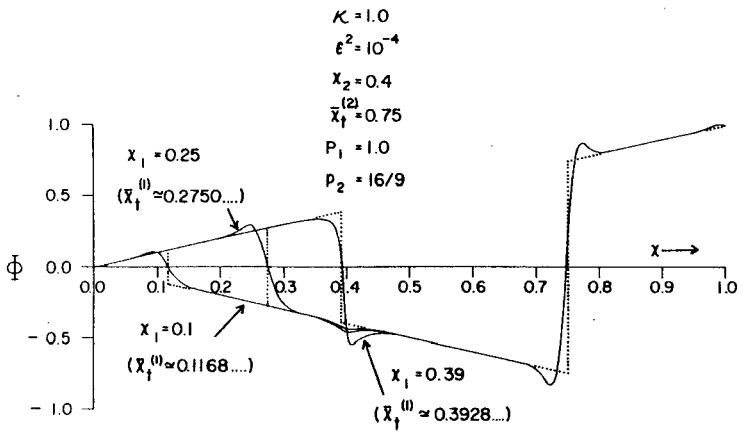

Figure 7. Distributions of Deformed Meridional Slope for Different Spreads of the External Ring Pressure Distribution

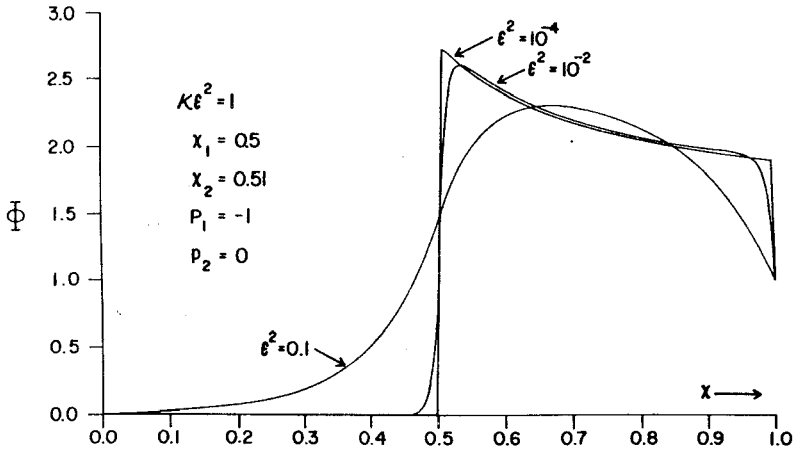

Figure 8. Distributions of Deformed Meridional Slope for Shells with Different Thickness Parameter Values Subjected to the Same Internal Ring Pressure Distribution

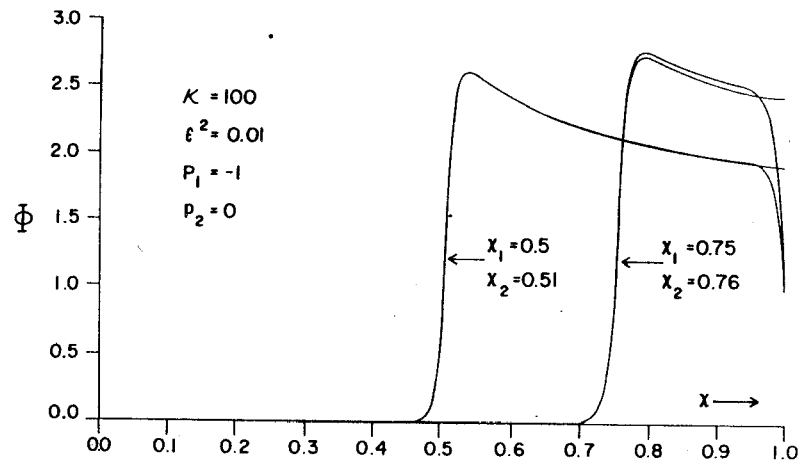

Figure 9. Distributions of Deformed Meridional Slope for Shells with a Clamped or Hinged Edge Subjected to an Internal Ring Pressure Distribution at Different Locations

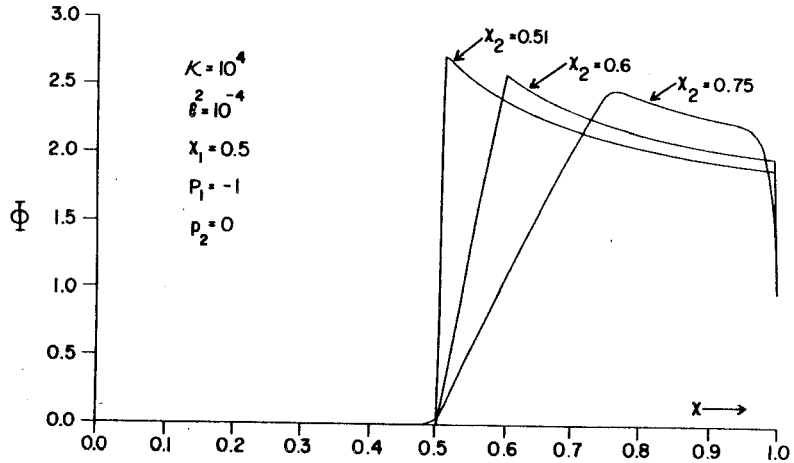

Figure 10. Distributions of the Deformed Meridional Slope for Shells Subjected to Internal Ring Pressure Distributions with the Same Resultant but Different Spreads